ECS Journal of Solid State Science and Technology, **2** (5) N93-N98 (2013)
2162-8769/2013/2(5)/N93/6/$31.00 © The Electrochemical Society

Mechanism of Modification of Fluorocarbon Polymer by Ultraviolet Irradiation in Oxygen Atmosphere

Quoc Toan Le,[a,z] Sergej Naumov,[b,*] Thierry Conard,[a] Alexis Franquet,[a] Matthias Müller,[c] Burkhard Beckhoff,[c] Christoph Adelmann,[a] Herbert Struyf,[a] Stefan De Gendt,[a,d,] and Mikhail R. Baklanov[a]**

[a]*IMEC, Leuven 3001, Belgium*
[b]*IOM-Leipzig, Leipzig 04318, Germany*
[c]*Physikalisch-Technische Bundesanstalt, X-ray and IR Spectrometry, Berlin 10587, Germany*
[d]*KULeuven, Leuven 3001, Belgium*

A fluorocarbon polymer generated by plasma polymerization of CF_4/CH_2F_2 used as a model polymer for sidewall residues was subjected to ultraviolet (UV) irradiation ($\lambda = 254$ nm). Fourier transform infrared spectroscopy and X-ray photoelectron spectroscopy indicated that the as-deposited fluorocarbon polymer mainly contains CF, CF_2, and a small concentration of unsaturated, fluorinated C=C bonds, and carbonyl functionalities. A partial removal of the polymer occurred during UV irradiation in oxygen. Experimental results showed that UV irradiation resulted in a slight decrease in fluorine content concomitant with the formation of carbonyl groups. The presence of reactive species such as oxygen during UV treatment (by production of singlet oxygen and radicals) was necessary to allow bond cleavage and an increase of hydrophilicity of the polymer fragments thus making the removal of the polymer possible in a subsequent wet clean. In terms of polymer bonding structure, the presence of C=C bonds and oxygen in the polymer backbone, in particular of C-O bonds, was crucial for light absorption at the wavelength used and played a key role in the bond scissioning process. Quantum chemical calculation was also performed to support the experimental results.
 [DOI: 10.1149/2.003305jss]

Manuscript submitted January 18, 2013; revised manuscript received February 18, 2013. Published March 2, 2013.

An important step in the back-end-of-line processing of advanced microelectronic CMOS integrated circuits consists in integrating thin copper interconnecting lines between active devices, such as transistors and capacitors. Copper lines are made in a damascene approach by locally etching dielectric layers using plasmas through a patterned photoresist layer and filling the transferred patterns with copper. During etching of porous dielectrics using fluorocarbon-containing plasmas such as CF_4, CH_2F_2, and C_4F_8, fluorocarbon polymers are formed and deposited on the created dielectric sidewalls.[1,2] These polymers are needed to ensure etching anisotropy, profile control and to minimize dielectric degradation. However, they must be removed afterwards to achieve high adhesion and good coverage of the material (metal) deposited in later process steps in the etched features. Unfortunately, it is known that this type of fluorocarbon polymer is chemically inert to many existing wet clean solutions, including aqueous solutions such as fluoride ion-containing or highly alkaline solutions, and solvent mixtures.[2] A short plasma treatment carried out prior to the wet clean step enhances the polymer removal efficiency but also has a drawback of irreversibly damaging the porous dielectrics.[3,4]

Recent studies have shown that exposing a fluorocarbon polymer formed by plasma polymerization to ultraviolet (UV) irradiation with a narrow band UV source of wavelength $\lambda = 254$ nm[2] or a broad band source of $\lambda \sim 200$–400 nm[5] with doses ≥ 3 J/cm^2 significantly modified the polymer film. This resulted in substantial removal ability in a subsequent wet clean process. For the fluorocarbon polymer generated using CF_4/CH_2F_2 plasma, it was also clear that a minimum amount/concentration of a reactive gas such as oxygen during the UV irradiation is required in order to achieve a complete removal of the polymer during the subsequent wet clean step. The results presented in this paper give further insight into the role played by UV irradiation and oxygen atmosphere in the modification of fluorocarbon polymer. Quantum chemical calculation was also performed to support the experimental results.

Experimental

In this study, plasma deposition of fluorocarbon polymer, referred to as CFx, was carried out on checkerboard wafer substrates by plasma polymerization of a CF_4/CH_2F_2/Ar gas mixture. A cross-section of three adjacent squares is shown in Figure 1. Briefly described, from bottom up the wafer is composed of Si substrate/low-*k* dielectric (90 nm, $k = 2.0$)/ bottom anti-reflective coating (BARC) (30 nm)/photoresist layer. Exposure was carried out through a checkerboard shadow mask, where the size of each square is 4×4 cm^2. Prior to polymer deposition, the BARC layer was first etched using CF_4 plasma (12 s), followed by the partial low-*k* etch using CF_4/CH_2F_2/Ar plasma (50 mTorr, 15 s) in a dual-frequency chamber (Lam Research Flex45). Under these conditions, the low-*k* layer remaining on the Si substrate was about 5 nm (ellipsometry data). A polymer layer was directly deposited on the entire wafer without stripping the remaining photoresist layer, using the same gas mixture and in the same chamber. For the polymer deposition step, CF_4/CH_2F_2 plasma (2:1 ratio) was applied to enhance polymer formation and deposition. The polymer thickness was measured to be about 60–70 nm. Only the low-*k* squares, i.e. polymer deposited on low-*k* surface, were used for this study.

The effect of UV photons and the ambient atmosphere (argon and oxygen) on the modification of CFx polymer was investigated using a UVO cleaner from Jelight Company, Inc., equipped with a single wavelength source ($\lambda = 254$ nm) generated by a low pressure mercury lamp. The power density of the light source was 25 mW/cm^2. In some experiments, two identical CFx samples were loaded into the chamber, where one was covered by a crystal filter having a wavelength cutoff of ~300 nm (SiO_2 containing B, Ba, Na, K, . . .) to investigate the

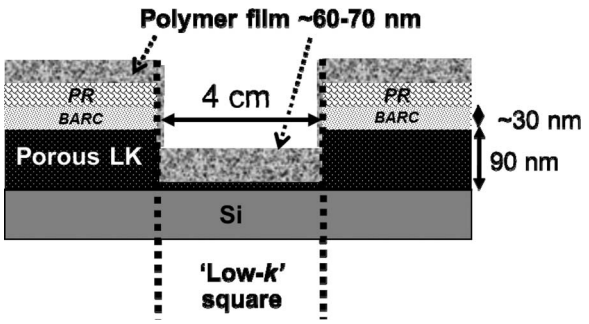

Figure 1. Cross-section of three adjacent squares in the checkerboard wafer. The samples used for the experiments described in this work consisted of the center-type square ('Low-*k*').

*Electrochemical Society Active Member.
**Electrochemical Society Fellow.
zE-mail: QuocToan.Le@imec.be

modification induced solely by reactive species such as radicals, without any effect of UV irradiation. Following the treatment, the UV source was extinguished and the chamber was continued to purge with the same gas under the same flow rate for 3 min. The samples were then transferred in air to X-ray photoelectron spectroscopy (XPS) and Time-of-flight secondary ions spectrometry (Tof-SIMS) chambers for analysis. For Near-edge X-ray absorption fine structure spectroscopy (NEXAFS) analysis, following the treatment the samples were shipped to another lab (Physikalisch-Technische Bundesanstalt, X-ray and IR Spectrometry, Germany). The aging time for those samples is estimated to be about 5 days from the time of deposition or UV treatment. Other characterization techniques consisted of Fourier-transform infrared spectroscopy (FTIR), and spectroscopic ellipsometry (SE).

FTIR (Thermo Fisher Scientific) spectra were recorded within the range of 400 to 4000 cm^{-1} using transmission mode with a resolution better than 2 cm^{-1} and averaged over 64 scans. XPS measurements were carried out using a Thermo VG Scientific Theta 300 system equipped with an Al Kα source (1486.6 eV) and simultaneous detection of photoelectrons at take-off angles between 22 and 78 degrees. ToF-SIMS analyses were performed with a TOFSIMS IV instrument from ION-TOF GmbH. Both positive and negative ion profiles were measured in a dual beam configuration using a Ga (15 keV) gun for analysis and a Xe (350 eV) gun for sputtering. Depth profiles were measured in the non-interlaced mode. Effective charge compensation was obtained by using an electron flood gun. A bunched 15 keV Ga beam rastered over 100 × 100 μm and a 1 keV Xe beam rastered over 300 × 300 μm were used.

Results and Discussion

Experimental results obtained from FTIR (Figure 2a) indicated that the polymer is mainly composed of C-F (stretching vibration, at ∼1090 and 1340 cm^{-1}) and CF_2 groups (doublet at 1160 and 1220 cm^{-1}). The absorption band centered at ∼1730 cm^{-1} can be assigned to double bonds in the form of C=C, –CF=CF–, and –$CF=CF_2$,[6–8] and also C=O groups. The absorption band at ∼600–1000 cm^{-1} can be assigned to vibrational absorption of $–CF_3$ and amorphous $–CF_2–$network.[6,9,10] Note that C-O groups, typically absorb between 1000–1300 cm^{-1}, could also be present in the polymer structure but might not be detected by FTIR in this case due to the strong absorption band of CFx groups. The absence of absorption bands at ∼2900–3000 cm^{-1} in the FTIR spectrum indicates that the polymer film does not contain C-H bonds, or at most they are at very low concentration, but it is composed almost exclusively of C-F, CF_2, CF=CF, $CF=CF_2$, C=O, and possibly C-O bonds. Complementary characterization of the CFx films was provided by XPS analyses. The C1s core-level spectrum recorded on the polymer (Figure 2b) confirmed the FTIR results and gave further insight into the polymer composition. Besides the presence of CF and CF_2 groups, there was also a small concentration of CF_3 groups. Table I summarizes the film composition (expressed as at.%), F/C and O/C ratios for both the as-deposited and UV-treated polymer films. The polymer deposited by plasma polymerization is highly reactive, which explains the incorporation of oxygen in the film and/or at the film surface during air exposure after the deposition step. Upon UV treatment in oxygen atmosphere, the concentration in oxygen significantly increased as shown in Table I.

Table I. XPS concentration (at.%), F/C, and O/C ratios calculated for the as-deposited fluorocarbon polymer and after UV treatment at various doses.

	C1s	F1s	O1s	Si2p	F/C	O/C
As-deposited	58.6	35.4	6.0	0	0.60	0.10
UV/3 $J.cm^{-2}$	59.5	30.1	10.4	0	0.51	0.17
UV/7.5 $J.cm^{-2}$	58.1	29.2	12.7	0	0.50	0.22

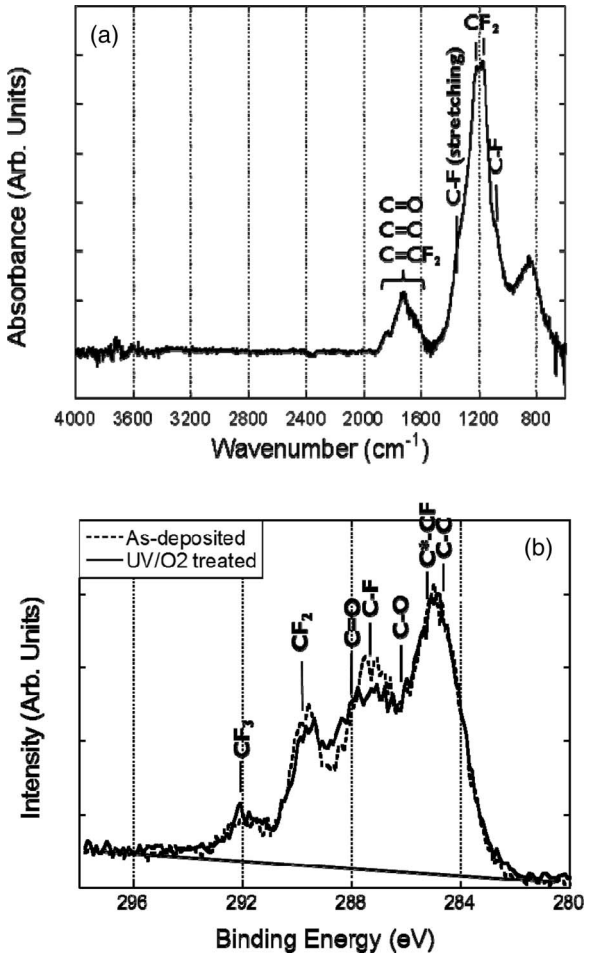

Figure 2. (a) FTIR spectrum of the as-deposited CFx model polymer generated by plasma polymerization using CF_4/CH_2F_2. (b) XPS C1s spectrum measured for the as-deposited CFx polymer and after UV/O_2 treatment for 5 min (7.5 J/cm^2).

The oxygen content of the film was measured to be about 6 at.% after deposition and increased to 12.7 at.% after UV treatment in O_2 atmosphere for 5 min (dose of 7.5 J/cm^2, Table I). The concentration in fluorine also slightly decreased after a 7.5 J/cm^2-UV treatment, from 35.4 to 29.2%. The change in the shape of the C1s core-level spectrum following the UV treatment gives a strong evidence that the loss in fluorine was mainly due to a drop in CF content concomitant with oxygen incorporation. The F/C ratio for the as-deposited polymer is much smaller with respect to the one measured for a linear fluorocarbon polymer such as polytetrafluoroethylene (PTFE, F/C = 2) or polyvinylidene fluoride (PVDF, F/C = 1). On the basis of FTIR and XPS results, a model bonding structure of the plasma-polymerized fluorocarbon polymer is proposed in Figure 3. Indeed, the absence of C-H bonds together with a low F/C ratio suggests that the as-deposited polymer does not (mainly) consist of linear polymer

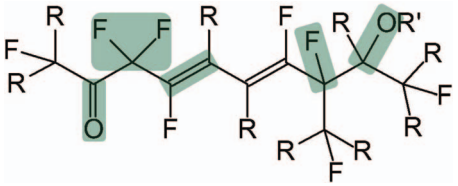

Figure 3. A proposed model of bonding structure for plasma-polymerized fluorocarbon polymer. R represents a branched, fluorinated carbon chain.

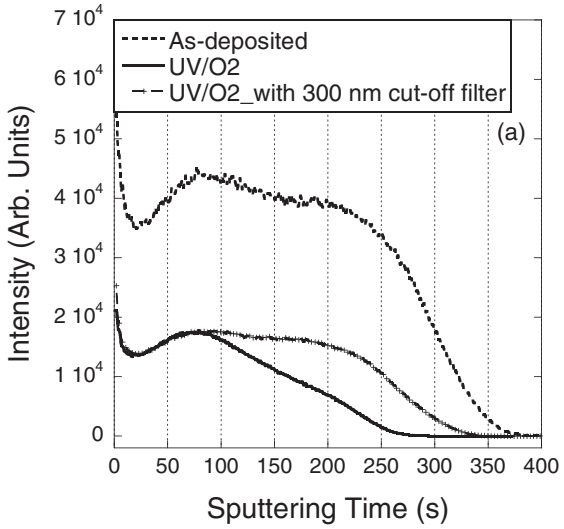

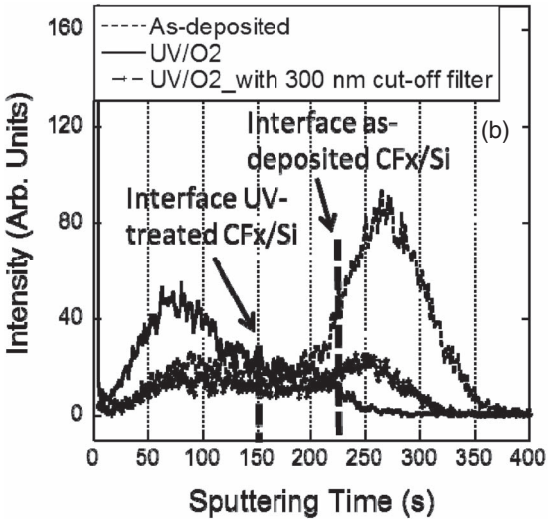

Figure 4. (a) F ToF-SIMS profiles (negative ions) for the as-deposited polymer and after UV treatment, with and without a UV cutoff filter at 300 nm. (b) O ToF-SIMS profiles (negative ions) for the as-deposited polymer and after UV treatment, with and without a UV cutoff filter at 300 nm.

chains but rather it is composed of significantly crosslinked networks. Crosslinked polymers formed by plasma polymerization are well documented in literature.[9,10] In fact, the degree of crosslinking reflects the magnitude of the formation of a three-dimensional network structure in the film, which tends to increase when the plasma gas mixture is diluted with Ar.[10] The fluorocarbon polymer also contains CF, CF_2, unsaturated, fluorinated C=C bonds, and carbonyl functionalities.

Figure 4a and Figure 4b display ToF-SIMS depth profiles obtained for the as-deposited and different UV-treated polymer samples. For UV treatments performed in oxygen atmosphere, defluorination and thickness decrease occurred during the UV irradiation (Figure 4a). Interestingly, for UV-treated polymers, the results showed that F (and CF) ion intensities were identical regardless of the presence or absence of the UV cutoff filter (Figure 4a). The only difference between the two UV-treated samples relies on the sample thickness, which is in good agreement with ellipsometry results (data not shown). The polymer film thickness significantly decreased when the polymer was directly exposed to UV irradiation, while it remained similar compared to the as-deposited film if a UV cutoff filter was used. This observation provides an evidence that a synergy of UV irradiation and oxygen etched the CFx polymer film, i.e. formation of volatile species, and also resulted in a defluorination of the remaining polymer layer. In

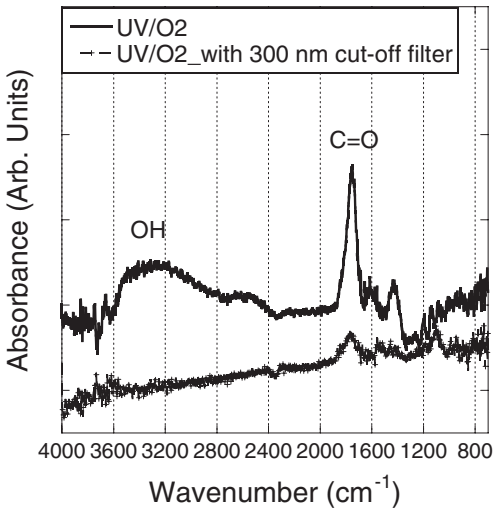

Figure 5. Differential FTIR spectra showing the formation of C=O bond (~1750 cm^{-1}) in the polymer film following the UV treatment in oxygen.

contrast, the thickness decrease was much less pronounced, almost non-existent, if the UV radiation is blocked by a cutoff filter of λ = 300 nm. For instance, under the UV filter a thickness decrease of ~ 1–2 nm was measured for a UV treatment of 5 min (corresponding to a dose of 7.5 J/cm^2 for a direct exposure). The slight decrease in thickness in the presence of the UV cutoff filter could be attributted to a loss in fluorine which was trapped in a planar structure of small graphite structure formed in the film.[10,11]

The O profiles shown in Figure 4b clearly indicate that oxygen incorporation occurred due to UV irradiation, where the maximum oxygen concentration was measured at ~19–25 nm from the film surface. Furthermore, the high-intensity oxygen ion measured close to the CFx/Si interface of the as-deposited film substantially reduced in intensity after the treatment in the absence of UV irradiation (UV-filtered sample). This result could be simply explained by the thermal effect during the UV irradiation for 5 min.

Figure 5 shows the *differential* FTIR spectra for the UV-treated polymers in the case of with and without a 300 nm cutoff filter. Note that the *differential* spectrum was obtained by subtracting the spectrum recorded after the UV treatment from the one before the treatment. The differential spectra are shown without baseline correction. The presence of the strong, positive absorption band at ~1750 cm^{-1} indicates the formation of C=O bonds in the polymer film caused by the UV irradiation in oxygen. In contrast, for the UV-filtered sample the intensity of that same absorption peak is substantially lower. In addition, the presence of an absorption peak centered at ~1600 cm^{-1} together with a much broader one between ~3100 and 3500 cm^{-1}, assigned to OH bonds, was also observed when the CFx polymer was directly exposed to the UV light.

The C1s NEXAFS spectra measured in grazing incidence geometry[12] on the as-deposited and UV-treated in oxygen are shown in Figure 6. The major peaks in the C1s region are located at ~285 eV (due to C1s to π^* C=C transitions) and 288.5 eV (C1s to σ^* C-H transitions). The absorptions originated from $C{=}CF_2$ (due to C1s to π^* $C{=}CF_2$ transitions), C-C (at 294 eV, C1s to σ^* C-C transitions) and C-F bonds (292 and 298 eV, C1s to σ^* C-F transitions)[13] are also expected but they might have been hidden by self-absorption effects[1] and the broad absorption band recorded between 289–298 eV. This broad absorption was commonly observed in the case of fluorocarbon polymers and was attributed to randomly oriented polymer chains.[14] Following UV irradiation, the presence of a clear, well-defined absorption peak located at ~286.5 eV gives a strong evidence of the for-

[1]The self-absorption effect causes damping and broadening of the fine structure resonances.

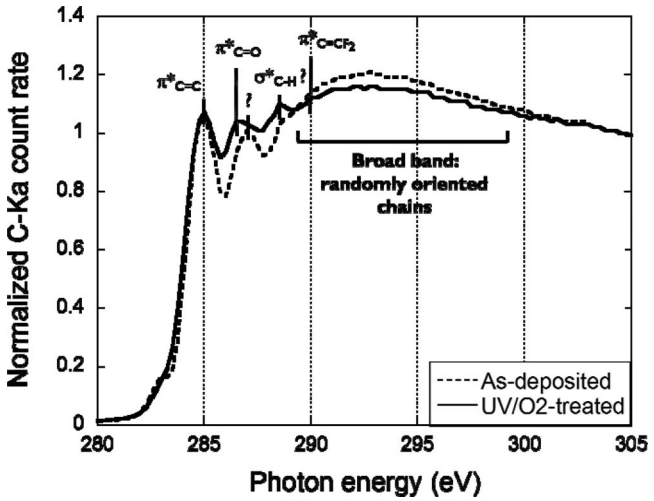

Figure 6. Comparison of NEXAFS spectra of the as-deposited CFx polymer generated by plasma polymerization using CF_4/CH_2F_2 and after UV/O_2 treatment.

mation of carbonyl caused by UV irradiation in oxygen atmosphere. The NEXAFS data confirm the FTIR and XPS results, and more importantly imply the chain scission by UV irradiation in oxygen. The formation of carbonyl groups and occurrence of chain scissioning process will be discussed in a later paragraph.

To support experimental results, parameters such as the electronic absorption spectra, energy levels of the excited states and the bond dissociation energies (BDE) Density Functional Theory (DFT) calculations on appropriate model molecule were carried out using the B3LYP[15–17] hybrid functional. The molecular geometries of all calculated molecules were optimized at the B3LYP/6–31G(d,p) level of theory (Gaussian 03 program).[18] Frequency calculations were done at the same level of theory to characterize the stationary points on the potential surface and to obtain zero point energies (ZPE) and Gibbs free energies (G) at a standard temperature of 298.15 K and a pressure of 1 atm using non-scaled vibrations. The relative stabilities of the different structures were calculated as the difference of the electronic energies ΔE_0 ($E_0 = E + ZPE$) and Gibbs free energies ΔG between the reactants and products relative to the ground state of the most stable structure of the model polymer (shown in Figure 7).

To test the possible influence of UV irradiation on the molecular structure and reaction parameters ΔE_0 and ΔG, geometry optimisations were carried out using self-consistent reaction field (SCRF) polarized continuum model CPCM.[19,20] The UV-Vis electronic transition spectra were calculated in vacuum with the Unrestricted Time Dependent (UTD DFT)[21] B3LYP/6–31 + G(d.p) method. Molecular orbitals (MOs) and UV-Vis spectra were visualized in graphical form with the help of ChemBio3D Ultra program.[22] The results of calculations obtained on model polymer are summarized in Figure 7.

Calculation of the energy of the first excited singlet state S^1 (196 kcal mol^{-1}) showed that photons with an energy of E >8.5 eV ($\lambda < 145$ nm) are required in order to excite the molecule. Relaxation by fast internal conversion shall lead to the S^1 state, which serves as a precursor for the subsequent intersystem crossing (ISC) into the excited triplet state T*. The energy of the lowest triplet state T^1 could not be calculated. Attempts to perform a geometry optimization for the triplet state were unsuccessful. Simulations running from the singlet state geometry as starting point did not converge into a stable triplet conformation, instead, immediate bond elongation of the C-F bond was observed. Thus, the QC calculations suggest that bond scission maybe faster than the relaxation of the excited triplet state T* into its T^1 ground state, or at least, that any triplet state is expected to be rather short-lived. Taking the λ_{max} of 154 nm as a rough measure of the triplet energy, this wavelength corresponds to ~188 kcal/mol.

In Figure 7, the bond dissociation energies (BDE) and ΔG are calculated as differences the electronic energies ΔE_0 and Gibbs free

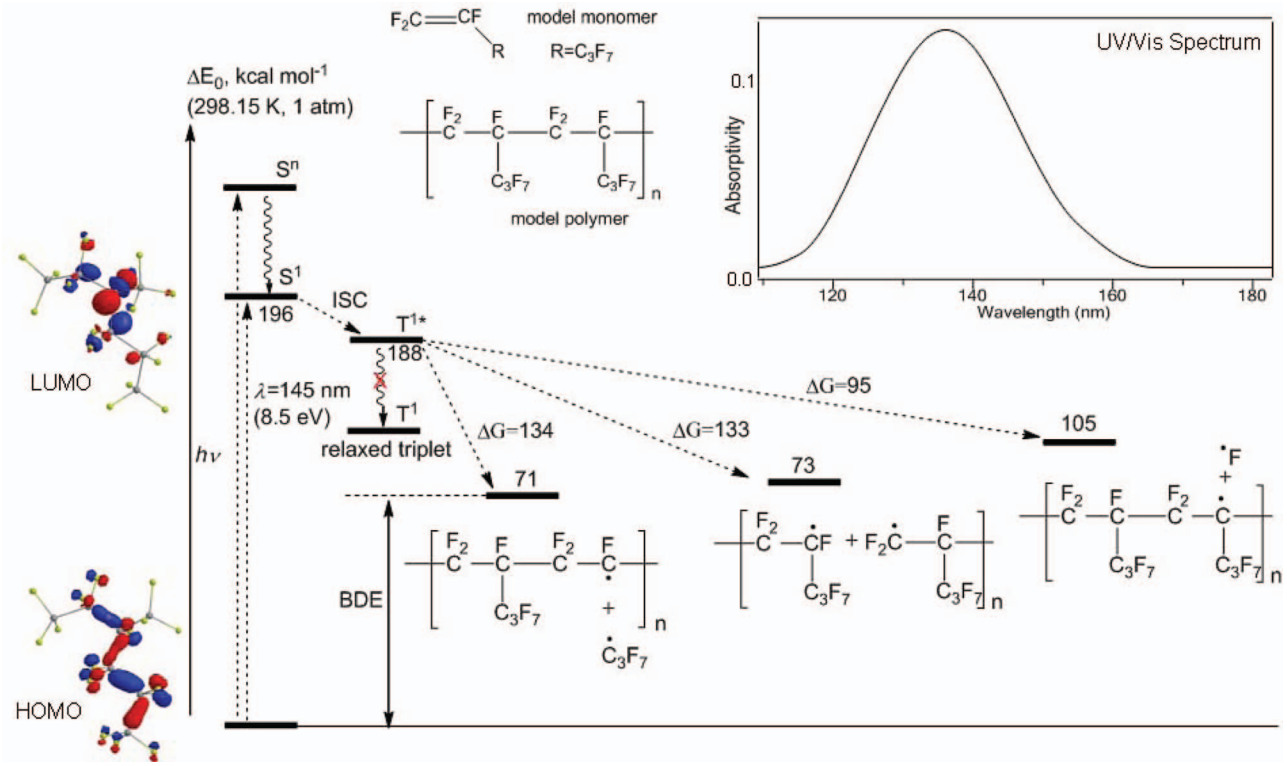

Figure 7. Quantum chemical calculations on the photolytical excitation of model polymer and possible fragmentation pathways. The calculated UV-Vis spectrum of model polymer is shown in the inset.

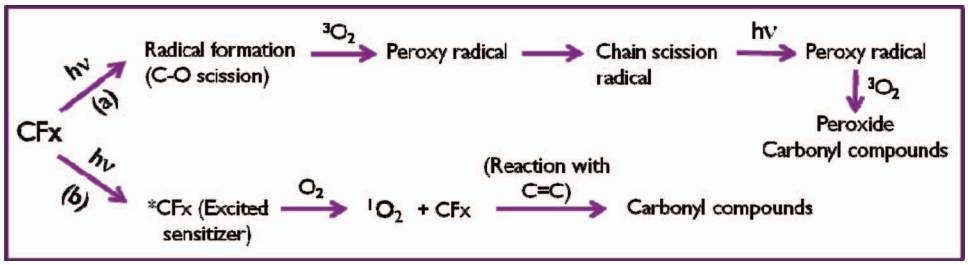

Figure 8. Proposed mechanism of formation of peroxyl and carbonyl groups via chain scissioning.

energies of the corresponding fragments respectively. As can be seen, all types of bonds present in the molecule may be subject to dissociation with respect to the excited triplet state. The C-C bond cleavage both from main and side chain of polymer is energetically more favorable than C-F cleavage. However, namely C-F bond cleavage was observed during attempts of optimization of model structure in the triplet state.

By comparing the highest occupied (HOMO) and lowest unoccupied (LUMO) orbitals (the latter can be taken as a first approximation of the electron distribution in the excited state) given in Figure 7, it is obvious that excitation leads to the strong intramolecular electron redistribution leading to essential change of calculated partial Mulliken atomic charges on C and F atoms. Thus, the partial charges in the ground state of +0.13 e and −0.27 e at C and F, respectively, change to −0.27 e (C) and –0.21 e (F) in the excited state. That indicates the reduced Coulomb attraction between these atoms, and therefore gives rise to a weakening of the corresponding C-F bond. Additionally, from the analysis of the electron distribution from MOs shown in Figure 7 it can be also seen that in the ground state the bonding σ-electron is delocalized mostly between C-C atoms. After excitation this σ-electron density will be removed from the C–C bonds and will be localized as an antibonding σ*-electron between C and F atoms, resulting in a weakening of the bond, facilitating the C-F bond cleavage. Thus, according to the calculations the reaction pathway may be based on both C-C and C-F bonds scission.

However, the calculated possible fragmentation pathways of the model polymer above after excitation cannot explain the experimental degradation observed for CFx polymer caused by lower energy UV treatment (λ >200 nm). A similar calculation was later performed using F_2C=CF bonds-containing structure as model polymer showing that the calculated energy of the first excited singlet state S^1 decreased to 6.3 eV (to be compared to 8.5 eV for the first model above) due to π−π* transition of electrons from double bonds. This represents a shift of ∼50 nm to lower energy.

The radicals formed after different bond scission within relative rigid polymer cage can undergo easy recombination. To learn more about the observed positive effect of the oxygen atmosphere on the decay of polymer after irradiation, the possible reactions of different radicals of the model polymer formed after excitation with molecular oxygen molecules in triplet state were studied. As calculated, radicals formed after scission of both C-F and C-C bonds react exothermic with $^3O_2$ ($\Delta H = -11$ kcal mol^{-1} and $\Delta H = -31$ kcal mol^{-1} for C-F and C-C bonds respectively). In both cases relative stable peroxyl radicals will be formed, which do not react further ($\Delta H = +70$ kcal mol^{-1}) with the polymer, thus preventing recombination of radicals generated after polymer chain scission that forms crosslinked networks.

Because of their electronic configuration, pure fluorocarbon polymers do not absorb in the UV light range above wavelengths of ∼200 nm.[23] Likewise, the calculated UV-Vis spectrum of the model molecule presented in Figure 7 shows a strong absorption at ∼140 nm. In our case, however, experimental results showed that the plasma-deposited CFx film has a good absorption within a range of 200–250 nm, indicating that the deposited polymer is not composed of only single C-F bonds, but also of other functional groups. Indeed, the FTIR and XPS data presented above showed that the polymer deposited by plasma polymerization consists of a complex, crosslinked structure including C=C, different CFx and also oxygen-containing groups. The calculation shown above together with the data in literature[24] suggest that for C-C and especially C-F bonds, a direct bond breaking caused by 254 nm UV light is not likely due to its relatively low energy (∼4.88 eV).

The presence of C=C bonds and in particular of oxygen in the polymer structure and in the treatment atmosphere appears to be crucial in the chain scissioning process. In such polymers, the excitation energy is significant lower than that of pure fluorocarbon polymer. This activation energy level is low enough such that the polymer molecule can be excited by photons with wavelengths >200 nm. The main modification processes are proposed in Figure 8. The reaction started with a radical formation as a result of a chain scission, which then reacted to oxygen giving peroxy radical and peroxide species (path a). For instance, scissioning of a C-O bond in the structure described in Figure 3 under UV irradiation led to the formation of –C*F radical, which resulted in the formation of peroxy radical, –CF(OO*), in the presence of oxygen.[25] Such radicals are then in turn converted to chain scission radicals due to UV light irradiation. Under oxygen atmosphere, chain scission peroxy radicals – and peroxides are finally formed. Peroxide compounds are able to decompose, in particular under UV irradiation, to different species, including carbonyl groups together with main chain scission to form fragments of smaller molecular weights. Furthermore, as shown by Dixon et al. for some model compounds of PTFE,[24] the bond energies for the C-C and C-F bonds presented in a radical are substantially lower with respect to those of the same types of bonds in a neutral molecule. As a consequence, the radicals formed as a result of direct UV irradiation (pathway a) initiate a number of C-C and C-F bond scission in the radical fragment. The second possibility (pathway b) consists of the formation of singlet oxygen, $^1O_2$, by energy transfer to oxygen from an excited photosensitizer,[26,27] where the fluorocarbon polymer played the role of the photosensitizer (light-absorbing substance). Singlet oxygen in turn reacts with C=C bonds in the polymer resulted, ultimately, in the cleavage of the olefin leading to carbonyl compounds following a reaction sequence similar to pathway a.

Summary

In summary, we have characterized fluorocarbon polymers after UV treatments in oxygen atmosphere using both bulk and surface sensitive techniques including FTIR, NEXAFS, XPS, and ToF-SIMS. Experimental results showed that UV irradiation of this polymer resulted in a slight decrease in fluorine content concomitant with the incorporation of oxygen, which gives a strong evidence of bond cleavage during the UV exposure. Furthermore, calculation of the energy of the first excited singlet state ^1S showed that photons with energies above 8.5 eV (λ < 145 nm) are required in order to excite –[CF_2-$CF(C_3F_7)$-CF_2-$CF(C_3F_7)$]- molecule. Energies provided by photons with λ > 200 nm, especially with λ = 254 nm, appeared not sufficient to excite this type of molecule leading to breaking of C-C and C-F bonds. In contrast, the presence of C=C bonds and oxygen in the polymer structure, in particular of C-O bonds, together with the formation of oxygen radicals under UV irradiation played a key role in bond scissioning process.

The use of a UV cutoff filter at 300 nm allowed separating the effect of UV irradiation from the chemical effect, i.e. oxygen radicals formed under UV on the modification of the polymer film. The results presented above demonstrate that the mechanism of fluorocarbon polymer modification involves a strong synergy between UV irradiation and the presence of oxygen in the treatment atmosphere. Three important conditions are required here to obtain a beneficial effect in terms of fluorocarbon polymer removal. First, polymer molecules should contain C=C or C-O bonds such that they can play the role of photosensitizer and allow initiating bond scissioning process. Second, the presence of oxygen in the ambient gas is required to generate reactive oxygen species resulting in the cleavage of C=C bonds and formation of carbonyl compounds. And third, UV irradiation dose should be high enough to create sufficiently small polymer fragments of low molecular weights such that they are able to be dissolved in subsequent wet clean solution.

Acknowledgments

The authors thank Prof. H. Fukumura (Tohoku University, Japan) and Dr. G. Vereecke (imec, Belgium) for fruitful discussion on reaction mechanism, and Dr. F. Holsteyns (imec) for reviewing the manuscript.

References

1. M. Darnon, T. Chevolleau, D. Eon, R. Bouyssou, B. Pelissier, L. Vallier, O. Joubert, N. Posseme, T. David, F. Bailly, and J. Torres, *Microelectron. Eng.*, **85**, 2226 (2008).
2. Q. T. Le, J.-F. de Marneffe, T. Conard, I. Vaesen, H. Struyf, and G. Vereecke, *J. Electrochem. Soc.*, **159**, H208 (2012).
3. N. Posseme, T. Chevolleau, O. Joubert, V. Vallier, and N. Rochat, *J. Vac. Sci. Technol. B*, **22**, 2772 (2004); F. Bailly, T. David, T. Chevolleau, M. Darnon, N. Posseme, R. Bouyssou, J. Ducote, O. Joubert, and C. Cardinaud, *J. Appl. Phys.*, **108**, 014906 (2010).
4. Q. T. Le, J. Keldermans, N. Chiodarelli, E. Kesters, M. Lux, M. Claes, and G. Vereecke, *Jpn J. Appl. Phys.*, **47**, 6870 (2008).
5. Q. T. Le, I. Simms, H. Yue, I. Brown, E. Kesters, G. Vereecke, H. Struyf, and S. De Gendt, presentation at SPCC, Austin, Texas, submitted to *Microelectron. Eng.*, (2012).
6. K. P. Huang, P. Lin, and H. C. Shih, *J. Appl. Phys.*, **96**, 354 (2004).
7. X. Gu, T. Nemoto, A. Teramoto, T. Ito, and T. Ohmi, *J. Electrochem. Soc.*, **156**, H409 (2009).
8. T. Easwarakhanthan, D. Beyssen, L. Le Brizoual, and J. Bougdira, *J. Vac. Sci. Technol. A*, **24**, 1036 (2006).
9. Y. Kim, J.-H. Lee, K. J. Kim, and Y. Lee, *J. Vac. Sci. Technol. A*, **27**, 900 (2009).
10. C. Biloiu, I. A. Biloiu, Y. Sakai, Y. Suda, and A. Ohta, *J. Vac. Sci. Technol. A*, **22**, 13 (2004).
11. R. d'Agostinos, R. Lamendola, P. Favia, and A. Giquel, *J. Vac. Sci. Technol. A*, **12**, 308 (1994).
12. B. Beckhoff, R. Fliegauf, M. Kolbe, M. Müller, J. Weser, and G. Ulm, *Anal. Chem.*, **79**, 7873 (2007).
13. P. Hale, S. Turgeon, P. Horny, F. Lewis, N. Brack, G. Van Riessen, P. Pigram, and D. Mantovani, *Langmuir*, **24**, 7897 (2008).
14. D. G. Castner, K. B. Lewis, Jr., D. A. Fischer, B. D. Ratner, and J. L. Gland, *Langmuir*, **9**, 537 (1993).
15. A. D. Becke, *J. Chem. Phys.*, **98**, 5648 (1993).
16. A. D. Becke, *J. Chem. Phys.*, **104**, 1040 (1996).
17. C. T. Lee, W. T. Yang, and R. G. Parr, *Phys. Rev. B*, **37**, 785 (1988).
18. Gaussian 03, Revision B.02, M. J. Frisch, G. W. Trucks, H. B. Schlegel, G. E. Scuseria, M. A. Robb, J. R. Cheeseman, J. A. Montgomery, Jr., T. Vreven, K. N. Kudin, J. C. Burant, J. M. Millam, S. S. Iyengar, J. Tomasi, V. Barone, B. Mennucci, M. Cossi, G. Scalmani, N. Rega, G. A. Petersson, H. Nakatsuji, M. Hada, M. Ehara, K. Toyota, R. Fukuda, J. Hasegawa, M. Ishida, T. Nakajima, Y. Honda, O. Kitao, H. Nakai, M. Klene, X. Li, J. E. Knox, H. P. Hratchian, J. B. Cross, C. Adamo, J. Jaramillo, R. Gomperts, R. E. Stratmann, O. Yazyev, A. J. Austin, R. Cammi, C. Pomelli, J. W. Ochterski, P. Y. Ayala, K. Morokuma, G. A. Voth, P. Salvador, J. J. Dannenberg, V. G. Zakrzewski, S. Dapprich, A. D. Daniels, M. C. Strain, O. Farkas, D. K. Malick, A. D. Rabuck, K. Raghavachari, J. B. Foresman, J. V. Ortiz, Q. Cui, A. G. Baboul, S. Clifford, J. Cioslowski, B. B. Stefanov, G. Liu, A. Liashenko, P. Piskorz, I. Komaromi, R. L. Martin, D. J. Fox, T. Keith, M. A. Al-Laham, C. Y. Peng, A. Nanayakkara, M. Challacombe, P. M. W. Gill, B. Johnson, W. Chen, M. W. Wong, C. Gonzalez, and J. A. Pople, Gaussian, Inc., Pittsburgh PA, 2003.
19. V. Barone and M. Cossi, *J. Phys. Chem. A*, **102**, 1995 (1998).
20. A. Klamt and G. Schüürmann, *J. Chem. Soc., Perkin Trans.*, **2**, 799 (1993).
21. R. Bauernschmitt and R. Ahlrichs, *Chem. Phys. Lett.*, **256**, 454 (1996).
22. ChemBio3D Ultra, version 12.0, CambridgeSoft, 1986-2009.
23. J. F. Rabek, *Polymer Photodegradation – Mechanisms and Experimental Methods*, Chapman and Hall (1995).
24. D. A. Dixon, B. E. Smart, P. J. Krusic, and N. Matsuzawa, *J. Fluor. Chem.*, **72**, 209 (1995).
25. Y. Momose, Y. Tamura, M. Ogino, S. Okazaki, and M. Hirayama, *J. Vac. Sci. Technol. A*, **10**, 229 (1992).
26. C. S. Foote, *Tetrahedron*, **41**, 2221 (1985).
27. E. L. Clennan, *Tetrahedron*, **56**, 9151 (2000).